Available online at www.sciencedirect.com
ScienceDirect
Journal of Power Sources 160 (2006) 277–283
JOURNAL OF POWER SOURCES
www.elsevier.com/locate/jpowsour

A fractal permeability model for the gas diffusion layer of PEM fuel cells

Ying Shi [a,b], Jinsheng Xiao [a,c,*], Mu Pan [a], Runzhang Yuan [a]

[a] *State Key Laboratory of Advanced Technology for Materials Synthesis and Processing, Wuhan University of Technology, Hubei 430070, China*
[b] *School of Automation, Wuhan University of Technology, Hubei 430070, China*
[c] *School of Automotive Engineering, Wuhan University of Technology, Hubei 430070, China*

Received 24 November 2005; received in revised form 3 January 2006; accepted 6 January 2006
Available online 20 February 2006

Abstract

In this paper a fractal permeability model for the gas diffusion layer (GDL) of PEM fuel cells (PEMFCs) is presented. The model accounts for the actual microstructures of the GDL in terms of two fractal dimensions, one relating the size of the capillary flow pathways to their population and the other describing the tortuosity of the capillary pathways. In addition, the gas molecule effect is considered by using the Adzumi equation. The fractal permeability model is found to be a function of the tortuosity fractal dimension, pore area fractal dimension, sizes of pore and the effective porosity of porous medium without any empirical constants. mercury-intrusion porosimetry was used to measure the microstructures of the GDL. Based on scanning electron microscope (SEM) images, two fractal dimensions are determined by the box-counting method. To verify the validity of the model, the predicted permeability data of the present fractal model were compared with the experimental data supplied by Toray Inc. It is found that the permeability prediction of the model was in accordance with experimental data. This verifies the validity of the present fractal permeability model for the GDL.

Keywords: PEM fuel cells; Gas diffusion layer; Permeability; Fractal

1. Introduction

PEM fuel cells (PEMFCs) have a high efficiency, power density, reliability and a quick startup capability. They could have a wider use in spaceflight and military applications with a huge market potential for fuel cells electric utilities, automotive transportation and in portable equipment. In the simulations of PEMFCs, supposing that porous media including gas diffusion layer (GDL), catalyst layer and membrane are always homogeneous, diffusion, momentum and energy equations are solved together with macroscopic transport properties such as permeability, effective thermal, electronic conductivity and effective diffusion coefficient. Firstly, this assumption is wrong. In reality, the GDL, catalyst layer and the membrane are anisotropic. Secondly, it relates to the transport mechanisms of PEMFCs without consideration of the micro-geometry and connectivity of the chaotic pore spaces of actual porous media through which the transport takes place, and such simulations give limited direction for the correct design of PEMFCs. Since porous media are complex, there is no good way to represent their microstructures exactly. Thompson et al. [1] confirmed that the interspaces in real porous media have a fractal character through scanning electron microscope (SEM). This work tries to apply fractal theory to PEMFC modeling, and develops a fractal model of permeability, one of the transport characteristics of the GDL. This model considers the microstructures of porous media, and will help us better understand the heat and mass transport mechanisms in this porous layer of the PEMFC.

2. Research methods and fractal research of permeability

In this section, conventional research methods and fractal research progress on permeability are introduced.

Research methods of the permeability included experimental measurement, analytical solution and numerical simulation. Traditionally, determination of the permeability tensor is best accomplished through experimental measurements since many

* Corresponding author. Tel.: +86 131 1439 5196; fax: +86 27 8785 9223.
E-mail address: jsxiao@mail.whut.edu.cn (J. Xiao).

0378-7753/$ – see front matter © 2006 Elsevier B.V. All rights reserved.
doi:10.1016/j.jpowsour.2006.01.032

and various measurement techniques all yield consistent results. However, these measurements often require a large number of carefully controlled experiments and, in general, have no predictive capability (i.e., each new material must be handled on a case-by-case basis). As a consequence, analytical (for simple cases) or numerical predictions of the permeability have for the past few years been the goal of many researchers in the field of porous media flow.

The permeability prediction models are mainly of three types:

(a) Fitting the experimental data to a pure empirical formula with several empirical constants. These empirical constants usually do not have any specific physical meaning, and the constants gained by different people always differ in values, therefore lacking of consistency. For example:

Lei et al. [2] studied the relation between porosity and permeability of the grain bed, the empirical formula gotten from the experiment data is

$$K = 1.72 \times 10^4 d^{1.465} \phi^{4.69} \quad (1)$$

where d and ϕ are the grain diameter and porosity, respectively, Eq. (1) is applied to the range of $d = 0.1$–0.45 mm. There are three empirical constants: 1.72×10^4, 1.465 and 4.69, so it is obvious that they have no specific physical meaning.

Adler and Thovert [3] presented several empirical formulae for the permeability of real porous media, e.g. an empirical formula for a glass particle porous media is

$$K = 0.117 r_e^2 \phi^{4.57} \quad (2)$$

where r_e is the equivalent radius of glass particle, Eq. (2) is applied to the range from $\phi = 0.4$ to $\phi = 0.79$. There are also several empirical constants in Eq. (2).

(b) By specific ideal models and theoretical analysis, in which the relation between permeability and different parameters of the structures in the porous media can be derived, which is semi-empirical approach. Some numerical coefficients of these models must be confirmed by experiment for a specific porous medium.

The famous Kozeny–Carman equation is a typical example of semi-empirical formula, given by

$$K = \frac{\phi^{n+1}}{C(1-\phi)^n} \quad (3)$$

where the exponential n and constant C are called Kozeny–Carman constants, these two constants vary for different porous media.

(c) Pure theoretical formulas are derived from Darcy's law. They are only applied to an ideal structure (such as circinal capillary, rectangle channel, etc.) porous media, but not to the random and disorderly structure of real porous media.

In practical applications, hardly any porous media have an ideal structure. The transport character parameters of the porous media have been measured mainly by experiments or computed by numerical simulation over several decades, so how to decrease or eliminate these empirical constants is the subject that people in this field still work on.

A large number of reports indicate that the microstructures and pore size distributions of porous media have a fractal characteristic. Therefore, it is possible to obtain the permeability of porous media through fractal analysis of the pore structures. Many people have made great efforts to study fractal theories and develop their application; so far they have already made some progress.

Tyler and Wheatcraft [4] combined porous capillary channel models with the Van Genuchten empirical formula, and got the fractal model for the water content characteristic curve. Rieu and Sposito [5] introduced theoretical models of pore distribution based on a Sierpinski-type gasket. Perfect et al. [6] improved models put forward by Tyler, Wheatcraft, and Rieu, Sposito, and they got the relation between the water content and the pore pressure in porous media. Shepard [7] applied the Koch curve to the simulation of soil's pore distribution, and then got a hydraulic conductivity formula in the form of an exponential.

Adler and Thovert [3] made a numerical simulation analysis of the transport problems of fractal objects with geometrical seep models in early times. But the results did not have any connection with the fractal dimension, nor were they compared with experimental data. They were only connected with geometrical iterative times. Adler studied the transport character in porous media later, and considered that the permeability of porous media could be expressed as follows: $K = K(\phi, D_f, \ldots)$, where D_f is the fractal dimension. But the quantitative expression of permeability was not given in this paper.

Chen and Shi [8] raised a fractal permeability model of a porous soil media, and this model has four empirical constants. The area fractal dimension of the soil pore distribution reported in their paper is that $D_f < 1$. But according to basic fractal theories, $1 < D_f < 2$ in two-dimensional space and $2 < D_f < 3$ in three-dimensional space, so their results about the area fractal dimension is doubtful. Another shortcoming of their work is that they did not compare theoretical models to experimental results, so the validity of the models needs to be confirmed further. In their recent work, they improved the computation of the fractal dimension and got the fractal dimension D_f between 1 and 2, at the same time, the empirical constants decreased from 4 to 2.

Pitchumani and Ramakrishnan [9] presented a fractal analytical model for evaluating the permeability of a porous fibrous textile. This model has not any empirical constants, which is a great improvement, but their model is incorrect for disobeying the basic fractal theories.

Yu and Lee [10] deduced a general analytical solution model for a kind of porous fibrous textile

$$K = a_g H_g \frac{H_g/12 + \sqrt{k_\perp}/2}{A} \quad (4)$$

where α_g, H_g, A and $k_\perp$ are biggest pore area, pore height, unit area and transverse permeability of fasciculi, respectively. Although Eq. (4) has no empirical constants, it is not applicable to porous media with random and irregular structures in which flow cannot be simplified into one-dimensional Stokesian flows.

In their subsequent research work, a universal fractal analytical solution model of permeability for porous media was derived based on the Hagen–Poiseulle equation and Darcy's law. Their research objectives are particle porous media, such as grit and soil, so their model does not apply to the GDL of a PEMFC that is a fibrous and microporous medium.

In the following sections, we will first introduce the basic fractal characteristic analytical theories of the GDL in a PEMFC. Then the analytical solution model of permeability will be derived based on experiment research. Finally we will assess the validity of the models.

3. Fractal permeability model for GDL of PEMFC

We will introduce some basic concepts of the fractal theory first.

Scale relationship between the measurement of a fractal object $M(L)$ and the metrical yardstick L is as follows [11]:

$$M(L) \sim L^{D_f} \tag{5}$$

where D_f is the fractal dimension, $M(L)$ the quality, or volume, or area of the object or the curvilinear length and L is the scale.

Another character of the fractal object (such as pore, or islands in the Earth) is that the cumulative number N (for example, the number of pore) of the fractal object and pore size distribution are related by the equation [11]

$$N(L \geq \lambda) = \left(\frac{\lambda_{max}}{\lambda}\right)^{D_f} \tag{6}$$

where λ and λ_{max} are the pore size and the maximum pore size, respectively, as far as porous media are concerned. The first derivative of Eq. (6) with respect to λ can be written as

$$-dN = D_f \lambda_{max}^{D_f} \lambda^{-(D_f+1)}\, d\lambda \tag{7}$$

The number of pores whose sizes fall within the infinitesimal range λ to $\lambda + d\lambda$ is given by Eq. (7), and $-dN > 0$.

When liquids flow through the pores of porous medium, the capillaries may be tortuous. These tortuous capillaries could be expressed by fractal equation [12]

$$L_t(\lambda) = L_0^{D_T} \lambda^{1-D_T} \tag{8}$$

where D_T is the tortuosity fractal dimension, and lies in the range $1 < D_T < 2$, which represents the extent of convolutedness of capillary pathways for fluid flow through a medium. Note that for a straight capillary path $D_T = 1$, and a higher value of D_T corresponds to a highly tortuous capillary. The limiting case of $D_T = 2$ corresponds to a highly tortuous line that fills a plane. Let the diameter of a capillary in the medium be λ and its tortuous length along the flow direction be $L_t(\lambda)$. L_0 is representative length of channels. For a straight capillary, $L_t(\lambda) = L_0$.

In early research, we made mercury porosimetry and BET absorption experiments for the GDL and from the experimental data of mercury-intrusion porosimetry, two fractal dimensions were computed. The calculated results showed that linear regression of the experimental data is obvious and GDL has a fractal character, so fractal theories are effective in the analysis and evaluation of the pore distribution characteristic of the GDL.

In simulation of a PEMFC, the gas permeability diffusion in a GDL needs to be taken into account. According to the experimental data from mercury porosimetry, it can be seen that the pore diameters of the GDL range from 10^{-5} to 10^{-8} m, and most pore diameters are about 10^{-6} m. However, the mean free path of a gas molecule is about 10^{-7} m; thus, the Knudsen number ranges from about 10^{-2} to 10, so the slipstream of the gas molecule should be considered. The flow rate $q(\lambda)$ through a single tortuous capillary can be given by the Adzumi equation [13]

$$q(\lambda) = \frac{\pi}{128}\frac{\Delta p}{L_t(\lambda)}\frac{\lambda^4}{\mu} + \frac{\varepsilon}{6}\sqrt{\frac{2\pi RT}{M}}\frac{\lambda^3}{L_t(\lambda)}\frac{\Delta p}{p} \tag{9}$$

where μ is the viscosity of the fluid, Δp the pressure gradient and ε is the Adzumi constant which is a non-dimensional proportional fraction, it takes a value of 0.9 for one kind of gas and a value of 0.66 for a gaseous mixture. M is the gas molecular weight, and the gas constant R is 8.3143 J mol^{-1} K^{-1}.

Eqs. (6)–(9) form the basis of the present fractal permeability model for the GDL of a PEMFC, which we will derive as follows.

The total flow rate Q can be obtained by integrating the individual flow rate $q(\lambda)$ over the entire range of pore sizes from the minimum pore λ_{min} to the maximum pore λ_{max} in a unit cell. According to Eqs. (7) and (9), we have

$$Q = -\int_{\lambda_{min}}^{\lambda_{max}} q(\lambda)\, dN(\lambda) = \int_{\lambda_{min}}^{\lambda_{max}} \left(\frac{\pi}{128}\frac{\Delta p}{L_t(\lambda)}\frac{\lambda^4}{\mu} + \frac{\varepsilon}{6}\sqrt{\frac{2\pi RT}{M}}\frac{\lambda^3}{L_t(\lambda)}\frac{\Delta p}{p}\right) D_f \lambda_{max}^{D_f} \lambda^{-(D_f+1)}\, d\lambda \tag{10}$$

Substituting the definitions of $L_t(\lambda)$ into Eq. (10), we can get

$$\begin{aligned} Q &= \int_{\lambda_{min}}^{\lambda_{max}} \left(\frac{\pi\, \Delta p D_f \lambda_{max}^{D_f}}{128\mu L_0^{D_T}} \lambda^{2+D_T-D_f} + \frac{\varepsilon}{6}\sqrt{\frac{2\pi RT}{M}}\frac{\Delta p}{p}\frac{D_f \lambda_{max}^{D_f}}{L_0^{D_T}} \lambda^{1+D_T-D_f}\right) d\lambda \\ &= \frac{\pi\, \Delta p D_f \lambda_{max}^{D_f}}{128\mu L_0^{D_T}} \frac{1}{3+D_T-D_f} \lambda^{3+D_T-D_f}\Big|_{\lambda_{min}}^{\lambda_{max}} + \frac{\varepsilon}{6}\sqrt{\frac{2\pi RT}{M}}\frac{\Delta p}{p}\frac{D_f \lambda_{max}^{D_f}}{L_0^{D_T}} \frac{1}{2+D_T-D_f} \lambda^{2+D_T-D_f}\Big|_{\lambda_{min}}^{\lambda_{max}} \\ &= \frac{\pi\, \Delta p D_f \lambda_{max}^{D_f}}{128\mu L_0^{D_T}} \frac{1}{3+D_T-D_f} \lambda_{max}^{3+D_T-D_f} \left[1 - \left(\frac{\lambda_{min}}{\lambda_{max}}\right)^{3+D_T-D_f}\right] + \frac{\varepsilon}{6}\sqrt{\frac{2\pi RT}{M}}\frac{\Delta p}{p}\frac{D_f \lambda_{max}^{D_f}}{L_0^{D_T}} \\ &\quad \times \frac{1}{2+D_T-D_f} \lambda_{max}^{2+D_T-D_f} \left[1 - \left(\frac{\lambda_{min}}{\lambda_{max}}\right)^{2+D_T-D_f}\right] \end{aligned} \tag{11}$$

Using the Darcy's laws, the permeability of GDL could be written as

$$K = \frac{\mu L_0 Q}{\Delta p A} = \frac{\pi}{128}\frac{L_0^{1-D_T}}{A}\frac{D_f}{3+D_T-D_f}\lambda_{max}^{3+D_T} \times \left[1-\left(\frac{\lambda_{min}}{\lambda_{max}}\right)^{3+D_T-D_f}\right] + \frac{\varepsilon}{6}\sqrt{\frac{2\pi RT}{M}}\frac{\mu}{A}\frac{L_0^{1-D_T}}{p} \times \frac{D_f}{2+D_T-D_f}\lambda_{max}^{2+D_T}\left[1-\left(\frac{\lambda_{min}}{\lambda_{max}}\right)^{2+D_T-D_f}\right] \quad (12)$$

Let the first item of Eq. (12) be K_1, the second item K_2, then Eq. (12) becomes

$$K = K_1 + K_2 \quad (13)$$

In the two-dimensional space, due to $1<D_T<2$ and $1<D_f<2$, the exponents of $\lambda_{min}/\lambda_{max}$, $3+D_T-D_f>1$ and $2+D_T-D_f>1$, respectively, and because $\lambda_{min}/\lambda_{max}<10^{-2}$, Eq. (12) could be reduced to

$$K = \frac{\mu L_0 Q}{\Delta p A} = \frac{\pi}{128}\frac{L_0^{1-D_T}}{A}\frac{D_f}{3+D_T-D_f}\lambda_{max}^{3+D_T} + \frac{\varepsilon}{6}\sqrt{\frac{2\pi RT}{M}}\frac{\mu}{A}\frac{L_0^{1-D_T}}{p}\frac{D_f}{2+D_T-D_f}\lambda_{max}^{2+D_T} \quad (14)$$

Thus, K_1 can be gained by

$$K_1 = \frac{\pi}{128}\frac{L_0^{1-D_T}}{A}\frac{D_f}{3+D_T-D_f}\lambda_{max}^{3+D_T} \quad (15)$$

According to Eq. (11), the corresponding total flow rate Q_1 can be written as

$$Q_1 = \frac{\pi\,\Delta p D_f}{128\mu L_0^{D_T}}\frac{1}{3+D_T-D_f}\lambda_{max}^{3+D_T} \quad (16)$$

Eq. (15) indicates that the permeability K_1 is a function of the pore area fractal dimension D_f, the tortuosity fractal dimension D_T and structural parameters A, L_0 and λ_{max}. If a straight capillary model ($D_T=1$) is assumed, Eqs. (15) and (16) can be reduced to

$$Q_1 = \frac{\pi\,\Delta p}{128\mu L_0}\frac{D_f}{4-D_f}\lambda_{max}^4 \quad (17)$$

$$K_1 = \frac{\pi}{128}\frac{1}{A}\frac{D_f}{4-D_f}\lambda_{max}^4 \quad (18)$$

respectively. Eqs. (17) and (18) indicate that the flow rate Q_1 and permeability K_1 are very sensitive to the maximum pore size λ_{max}. It is also shown that a higher value of D_f corresponds to higher flow rate and higher permeability values. From Eqs. (17) and (18), we can see that the flow rate and the permeability will reach the possible maximum values as the pore area fractal dimension approaches its possible maximum value of 2. The limiting case of $D_f=2$ corresponds to a smooth surface or a plane or a compact cluster. This means that if we consider the smooth surface, compact cluster, circle or square to be the cross-section of a pore, the fractal dimension of the cross-section is 2 and the pore volume fraction of the cross-section is 1. Both the flow rate and the permeability are a maximum under such conditions. Thus, for flow through the unit cell with a single capillary tube or pore with $D_f=2$, we have the maximum flow rate and maximum permeability from Eqs. (17) and (18),

$$Q_{1\,max} = \frac{\pi\,\Delta p}{128\mu L_0}\lambda_{max}^4 = \frac{D_e^2}{32}\frac{A\,\Delta p}{L_0\mu} \quad (19)$$

$$K_{1\,max} = \frac{\pi}{128}\frac{1}{A}\lambda_{max}^4 = \frac{D_e^2}{32} \quad (20)$$

Eq. (19) is exactly the Hagen–Poiseulle equation [13], and the permeability value of $D_e^2/32$ is exactly the expression for flow through a pipe.

K_2 in Eq. (13) is the modified item when the Knudsen effect is taken into account, so the effect of K_2 on the total permeability is not very large, while the first item K_1 plays an important role in permeability computation. From Eqs. (19) and (20), it can be seen that our model is consistent with the physical situation. Therefore, one can find the flow rate and the permeability for flow through the unit cell with a straight capillary tube either from the modified Hagen–Poiseulle equation or from Eqs. (19) and (20) without consideration of the Knudsen effect.

As mentioned above, we can see that in Eq. (14), K_1 is the permeability expression that can be derived from the modified Hagen–Poiseulle equation and K_2 is the modified item caused by the molecule slipstream.

Subsequently the expression of the total area of the unit cell A will be derived by the definition of porosity as follows:

$$A_p = -\int_{min}^{max}\frac{1}{4}\pi\lambda^2\,dN(\lambda) = \int_{\lambda_{min}}^{\lambda_{max}}\frac{1}{4}\pi\lambda^2 D_f\lambda_{max}^{D_f}\lambda^{-(D_f+1)}\,d\lambda = \frac{1}{4}\pi D_f\lambda_{max}^{D_f}\frac{1}{2-D_f}\lambda^{2-D_f}\Big|_{\lambda_{min}}^{\lambda_{max}} = \frac{\pi D_f}{4(2-D_f)}\lambda_{max}^2\left[1-\left(\frac{\lambda_{min}}{\lambda_{max}}\right)^{2-D_f}\right] \quad (21)$$

where A_p is the pore area of the unit cell.

According to the definition of porosity, we get

$$\phi = \frac{A_p}{A} \Rightarrow A = \frac{A_p}{\phi} = \frac{\pi D_f\lambda_{max}^2}{4\phi(2-D_f)}\left[1-\left(\frac{\lambda_{min}}{\lambda_{max}}\right)^{2-D_f}\right] \quad (22)$$

where ϕ is the porosity.

Substituting Eq. (22) into Eq. (12), we have

$$K = \frac{1}{32}\frac{2-D_f}{3+D_T-D_f}\frac{L_0^{1-D_T}\lambda_{max}^{1+D_T}\phi}{[1-(\lambda_{min}/\lambda_{max})^{2-D_f}]} \times \left[1-\left(\frac{\lambda_{min}}{\lambda_{max}}\right)^{3+D_T-D_f}\right] + \frac{\varepsilon}{3}\sqrt{\frac{2RT}{\pi M}}\frac{\mu L_0^{1-D_T}}{p}\frac{(4-2D_f)\phi}{2+D_T-D_f}\frac{\lambda_{max}^{D_T}}{[1-(\lambda_{min}/\lambda_{max})^{2-D_f}]} \times \left[1-\left(\frac{\lambda_{min}}{\lambda_{max}}\right)^{2+D_T-D_f}\right] \quad (23)$$

In the two-dimensional space, Eq. (23) can be abbreviated to

$$K = \frac{1}{32}\frac{2-D_f}{3+D_T-D_f}\frac{L_0^{1-D_T}\lambda_{max}^{1+D_T}\phi}{[1-(\lambda_{min}/\lambda_{max})^{2-D_f}]} + \frac{\varepsilon}{3}\sqrt{\frac{2RT}{\pi M}}\frac{\mu L_0^{1-D_T}}{p}\frac{(4-2D_f)\phi}{2+D_T-D_f}\frac{\lambda_{max}^{D_T}}{[1-(\lambda_{min}/\lambda_{max})^{2-D_f}]} \quad (24)$$

Eqs. (23) and (24) without empirical constants are the analytical solution model of permeability for GDL. It can be seen that the permeability K is a function of two fractal dimensions D_f, D_T and porous material microstructure parameters. Eqs. (23) and (24) all have 11 parameters, and every parameter has specific physical meaning. So the permeability model gained by the fractal theories is obviously better than the well-known Konzeny–Carman equation from the viewpoint of describing a penetrative mechanism.

According to the following formula proved recently by Yu and Li [14]:

$$\phi = \left(\frac{\lambda_{min}}{\lambda_{max}}\right)^{d_E-D_f} \quad (25)$$

where d_E is Euclid dimension, and $d_E = 2$, $1 < D_f < 2$ in the two dimensional space; while $d_E = 3$, $2 < D_f < 3$ in the three dimension space. Eq. (24) can be further abbreviated to

$$K = \frac{1}{32}\frac{2-D_f}{3+D_T-D_f}\frac{L_0^{1-D_T}\lambda_{max}^{1+D_T}\phi}{1-\phi} + \frac{\varepsilon}{3}\sqrt{\frac{2RT}{\pi M}}\frac{\mu L_0^{1-D_T}}{p}\frac{(4-2D_f)\phi}{2+D_T-D_f}\frac{\lambda_{max}^{D_T}}{1-\phi} \quad (26)$$

In the following section, we will discuss the determination of two fractal dimensions D_f and D_T and fractal permeability prediction of GDL.

4. Two fractal dimensions evaluation and permeability prediction for the GDL

In the fractal analytical solution model of permeability, we need to determine two dimensions: the tortuosity fractal dimension D_T, which can be obtained using a box-counting method, and the pore area fractal dimension D_f.

The pore area fractal dimension can be determined by several methods, which can be roughly sorted into three types. Taking linear regression of the experimental data to gain the fractal dimension is the first method. Such experiments include mercury porosimetry and BET absorption. Processing the SEM images or the images from other imaging technology to compute the fractal dimension belongs to the second method. The most common method based on images is the box-counting method; furthermore, a difference box-counting method and a Sierpinski-type gasket or basket method can also be used. The method by analytical solution of the fractal dimension belongs to the third approach.

Using a box-counting method to process the SEM images of two samples: TGP-H-060 carbon paper and TGP-H-060 carbon paper treated with PTFE, we get the tortuosity dimension of two samples $D_T = 1.1447$, the pore area dimension of TGP-H-060 carbon paper $D_f = 1.9669$ and that of TGP-H-060 carbon paper treated with PTFE $D_f = 1.9276$.

Table 1
The microstructual parameters and operating parameters of samples

Parameter	Number one	Number two	Description
λ_{max}	8×10^{-5} m	7×10^{-5} m	Maximum pore diameter
λ_{min}	3.079×10^{-8} m	1.487×10^{-8} m	Minimum pore diameter
ϕ	0.55	0.78	Porosity
L_0	1.9×10^{-4} m	1.9×10^{-4} m	Gas diffusion layer thickness
μ	1.2×10^{-5} Pa s	1.2×10^{-5} Pa s	Hydrogen viscosity
p	1.01325×10^5 Pa	1.01325×10^5 Pa	Hydrogen pressure
T	353 K	353 K	Temperature

As follows, the prediction of permeability will be made when H_2 goes through two samples (number one sample is TGP-H-060 carbon paper and number two sample is TGP-H-060 carbon paper treated with PTFE). Table 1 gives the operating parameters and some experimental data from mercury porosimetry.

We now compare the permeability values based on the present fractal model with the reference value supplied by Toray Inc. for the number one sample. The results are presented in Fig. 1.

The real line in Fig. 1 shows that the fractal permeability model for the number one sample is slightly lower than the reference value, that is, 8×10^{-8} m^2. In the same figure, we also plot the well-known Kozeny–Carman equation given by Eq. (3), in which $C = 180/\lambda_{mean}^2$, $\phi = 0.78$, the mean pore diameter λ_{mean} is computed by experimental data from mercury porosimetry. It is shown that the present fractal permeability model is in better agreement with the reference value than the Kozeny–Carman equation. Moreover, we forecasted the permeability of TGP-H-060 carbon paper treated with PTFE by our fractal model and Kozeny–Carman equation, respectively, also shown in Fig. 1.

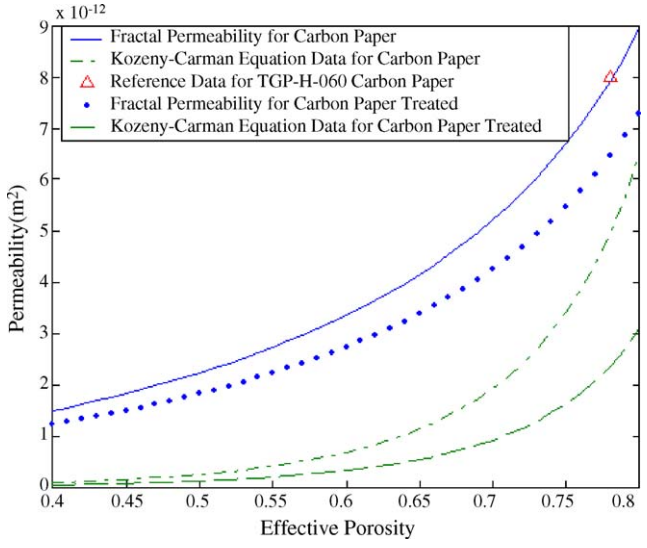

Fig. 1. A comparison of permeability from the present fractal model and Kozeny–Carman equation.

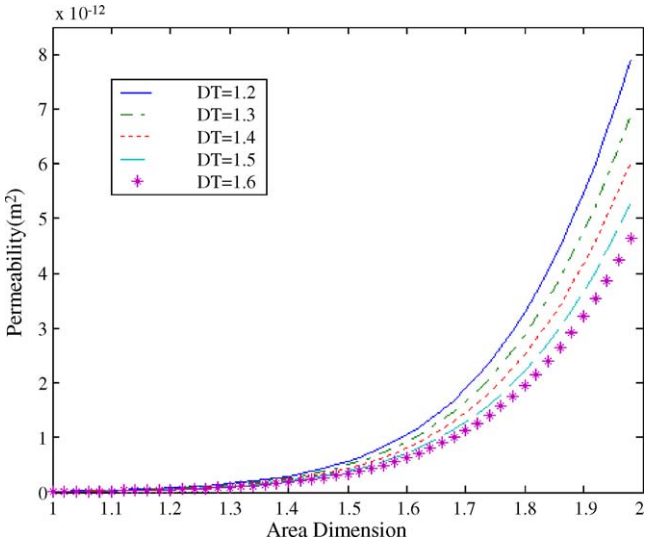

Fig. 2. Effect of D_f and D_T on permeability for carbon paper.

From the results, it can be seen that because the porosity of carbon paper descends and the pore space decreases after being treated by PTFE, the corresponding permeability decreases with respect to that of carbon paper without treatment.

The effects of the pore area dimension D_f, the tortuosity dimension D_T and porosity ϕ on the permeability are plotted in Figs. 2 and 3. Fig. 2 shows the permeability variation with the pore area dimension D_f for different values of the tortuosity dimension D_T. It is seen that the permeability increases as D_f increases. Increase in D_f corresponds to increase in the number of the larger pores, and decrease in the population of the smaller pores within a representative carbon paper volume. The resulting augmentation in the available area for gas flow in turn leads to an increase in the permeability.

An interesting fact can be elucidated from Fig. 2 which is that for any tortuosity dimension, as the pore area dimension D_f approaches its largest possible value of 2, the permeability approaches maximum possible values as mentioned above. This theoretical limit on D_f corresponds to the situation wherein the carbon paper entirely consists of pores and does not contain any solid matrix. Under such a condition, the flow-through porous medium whose porosity approaches unity becomes the flow through a zone. Moreover, when the pore area dimension D_f approaches its lowest possible value of 1, the permeability approaches minimum possible values. Its theoretical limit on D_f corresponds to the situation wherein the carbon paper consists of pores of sizes approaching zero, which no longer contributes to the gas flow.

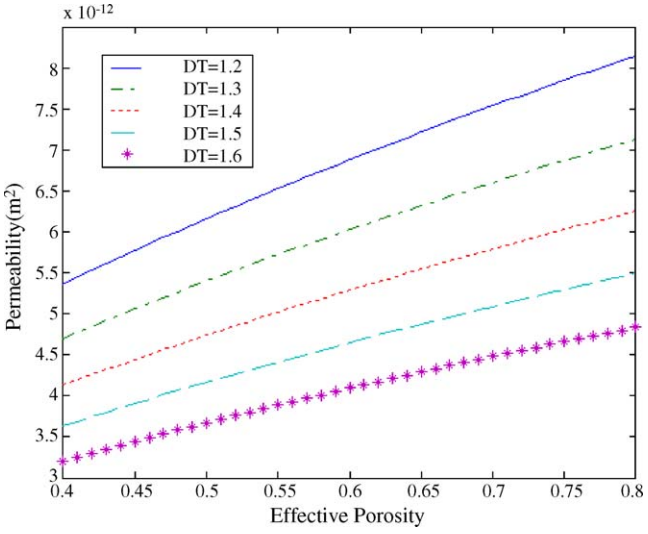

Fig. 3. Effect of D_T and effective porosity on permeability for carbon paper.

The variation of the permeability with porosity ϕ and the tortuosity dimension D_T is presented in Fig. 3. The permeability is seen to decrease with increasing the tortuosity dimension. The decrease in permeability with the increase in D_T is attributed to the increased flow resistance due to the highly convoluted capillary pathways. Furthermore, the permeability increases with rising porosity in the carbon paper owing to increase in the available pore volume for the gas to permeate through, which is also observed in Fig. 2.

The effect of K_2 on the total permeability is also studied with the ratio of K_2 to the total permeability K. The results show that the ratios lie in the range from 0.29 to 0.34% for carbon paper and from 0.33 to 0.38% for carbon paper treated with PTFE. The values of K_2/K are so small that we can ignore K_2 in the permeability computation, which indicates little reaction of the Knudsen effect to the flow through carbon paper, so the modified items of Eqs. (23), (24) and (26) need not be taken into account in permeation through carbon paper. In addition, the ratios of K_2 to the total permeability K of the number two sample are greater than that of the number one sample for the mean pore size of the number two sample is smaller than that of number one.

5. Conclusion

In this paper, the relationship between the microstructure and the permeability of the GDL in a PEMFC was given. With the microstructural parameters including two fractal dimensions of porous medium, the smallest and biggest pore diameter and porosity we could predict the corresponding permeability through fractal models. The analytical solution permeability model of the GDL does not have any empirical constants, and every parameter in this model has a specific physical meaning. So the permeability model gained by fractal theory is obviously better than the well-known Konzeny–Carman equation from the viewpoint of describing a penetrative mechanism. The prediction results show that the present fractal permeability model is in better agreement with the reference value than the Kozeny–Carman equation.

The effects of the area dimension D_f, the tortuosity dimension D_T and porosity ϕ on the permeability are discussed in detail. And we can draw the conclusion that permeability increases as D_f or ϕ increases, or as D_T decreases.

Therefore, using fractal geometrical theories to study the pore structures of the GDL in a PEMFC provides a new research method for the gas transport mechanism in the simulation of PEMFCs. It makes quantitative analysis of the relationship

between the micro-mechanism and the macroscopical material parameters of a GDL possible.

Acknowledgment

The authors acknowledge the financial support of the Special Scientific Research Foundation for College Doctor Subjects from Ministry of Education of China (No. 20030497012 and No. 20050497014).

References

[1] A.H. Thompson, A.J. Katz, C.E. Krohn, Adv. Phys. 36 (5) (1987) 625.
[2] S.Y. Lei, L.Q. Wang, L.Q. Jia, C.M. Xia, J. Tsinghua Univ. 38 (5) (1998) 20.
[3] P.M. Adler, J.F. Thovert, Appl. Mech. Rev. 51 (9) (1998) 537.
[4] S.W. Tyler, S.W. Wheatcraft, Water Resour. Res. 26 (1990) 1047.
[5] M. Rieu, G. Sposito, Soil Sci. Soc. Am. J. 55 (1991) 1231.
[6] E. Perfect, N.B. Mclaughlin, B.D. Kay, G.C. Topp, Water Resour. Res. 32 (2) (1996) 281.
[7] S.J. Shepard, Soil Sci. Soc. Am. J. 57 (1993) 300.
[8] Y.P. Chen, M.H. Shi, J. Tsinghua Univ. 40 (12) (2001) 94.
[9] R. Pitchumani, B. Ramakrishnan, Int. J. Heat Mass Transfer 42 (1999) 2219.
[10] B.M. Yu, L.J. Lee, Polym. Compos. 21 (5) (2000) 660.
[11] B.B. Mandelbrot, The Fractal Geometry of Nature, Freeman, San Francisco, USA, 1982.
[12] S.W. Wheatcraft, S.W. Tyler, Water Resour. Res. 24 (1988) 566.
[13] D.E. Xue, H.X. Wang, C.S. Zhang, S.S. Xun, Permeation Physics in Porous Media, Petroleum Industry Publishing Company, Beijing, 1982.
[14] B.M. Yu, J.H. Li, Fractals 9 (3) (2001) 365.